Diversity and BER Performance of Zak-OTFS Modulation

Fathima Jesbin, Jaswanth Bodempudi and A. Chockalingam
Department of ECE, Indian Institute of Science, Bangalore

***Abstract*—Zak-OTFS is a promising modulation scheme for 6G and beyond due to its enhanced resilience to high Dopplers and its structured input-output relation through twisted convolution operation. In this paper, we analyze the diversity performance of Zak-OTFS under maximum-likelihood (ML) detection and perfect delay-Doppler (DD) domain channel state information (CSI). Our analysis provides a condition in the design of pulse shaping filters to achieve full DD domain diversity. Our results show that sinc and Gaussian filters achieve full DD diversity in Zak-OTFS. This is in contrast with the widely investigated multicarrier (MC) version of OTFS (MC-OTFS), whose diversity order is one and requires phase rotation operation on the transmit vector to achieve full DD diversity. Further, we analyze the bit error performance of Zak-OTFS under imperfect CSI. We carry out the analysis for 1) the mismatched ML detector, where the channel matrix in the conventional ML decision rule is replaced with the estimated channel matrix, and 2) the true ML detector which takes into account the CSI error statistics in the ML decision rule, and quantify the performance gap between the two detectors.**

***Index Terms*—Zak-OTFS modulation, delay-Doppler domain, doubly-selective channels, diversity analysis, imperfect CSI.**

I. Introduction

The advent of 6G heralds a transformative era in wireless communication, promising advanced applications and ultra-reliable, low-latency connectivity. This paradigm shift faces challenges posed by complex channel conditions arising from high mobility, high carrier frequencies, and dense urban environments. These conditions lead to significant time selectivity in the channel, necessitating the exploration of advanced technologies, including novel modulation schemes, for robust communication. Orthogonal time frequency space (OTFS) modulation introduced in [1] and extensively researched later [2] offers a potential solution to effectively mitigate rapid time variations in the channel. Its superior performance is attributed to two key features: multiplexing of information symbols in the delay-Doppler (DD) domain and DD channel parameterization, which render a sparse and predominantly time-invariant representation. These features facilitate reduced complexity and pilot overhead in DD channel estimation, and better equalization.

The initial focus of OTFS research was on multicarrier OTFS (MC-OTFS), which employs a two-step conversion between DD domain and time domain (TD) via time-frequency (TF) domain [1],[2]. The popularity of the MC-OTFS stems from its easy integration into existing MC schemes, with pre- and post-processing operations. Recently, a single-step conversion approach based on Zak transform theory [3], named Zak-OTFS, is gaining prominence due to its strong mathematical foundation, structured input-output relation (through twisted convolution operation), and augmented resilience to high Doppler [4]-[10]. These advantages position Zak-OTFS as an attractive candidate to meet the modulation requirements of 6G and beyond.

Recent references [5], [6] highlight the salient features of Zak-OTFS, especially its *non-fading* channel interaction and *predictability* of the input-output relation, and offer guidance on their practical implications. These attributes are attributed to the better localization of the Zak-OTFS waveform, which is a quasi-periodic pulse in the DD domain confined within its fundamental DD period (pulsone in time domain). The concept of the *crystalline regime* has also been introduced, wherein the DD periods of the waveform exceed the effective DD channel spreads caused by the physical doubly-spread channel and the pulse shaping filters. Operating in this regime alleviates the issue of DD domain aliasing, yielding robust performance.

In this paper, we focus on the DD diversity performance of Zak-OTFS, which has not yet been addressed in the literature. In this regard, we note that diversity analysis for MC-OTFS in [11] showed that the DD diversity order achieved in MC-OTFS is one and that phase rotation on the transmit vector is required to achieve full DD diversity. In contrast, our analysis and results in this paper show that Zak-OTFS achieves full DD diversity. We also analyze the performance of Zak-OTFS with imperfect channel state information (CSI). Our contributions in this paper can be summarized as follows.

- First, we analyze the diversity performance of Zak-OTFS under maximum-likelihood (ML) detection and perfect CSI. We obtain a condition on the design of transmit and receive pulse shaping filters for achieving the full DD domain diversity. Our simulation results show that sinc and Gaussian filters achieve full DD diversity.
- Second, we analyze the bit error performance of Zak-OTFS under imperfect CSI. We carry out the analysis for 1) the mismatched ML detector, where the channel matrix in the conventional ML decision rule is replaced with the estimated channel matrix, and 2) the true ML detector which takes into account the CSI error statistics, and quantify the performance gap between the two detectors.

II. Zak-OTFS system model

Figure 1 presents block diagram of the transceiver signal processing in Zak-OTFS. Zak transform operation is central to Zak-OTFS, converting a time-domain (TD) signal into a DD signal with quasi-periodic structure. This transform is parameterized by delay period (τ_p) and Doppler period

This work was supported in part by the J. C. Bose National Fellowship, Department of Science and Technology, Government of India.

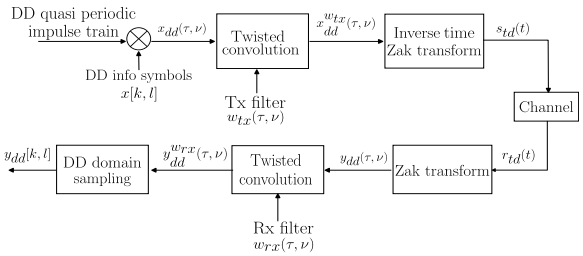

Fig. 1: Transceiver signal processing in Zak-OTFS.

(ν_p) which are inversely related ($\tau_p\nu_p = 1$). Zak-OTFS waveform is a quasi-periodic pulse in the DD domain, localized within fundamental DD period defined as $\mathcal{D}_0 \triangleq \{(\tau,\nu): 0 \le \tau < \tau_p, 0 \le \nu < \nu_p\}$, where τ and ν denote the delay and Doppler variables, respectively. Conversion to TD using the inverse time-Zak transform yields a pulse train modulated by a frequency tone, referred to as a *pulsone*. These DD pulses are located on the information lattice defined as

$$\Lambda_{\rm dd} \triangleq \Big\{\Big(k\frac{\tau_p}{M}, l\frac{\nu_p}{N}\Big) : k,l \in \mathbb{Z}\Big\}. \tag{1}$$

Here $M = B\tau_p$ and $N = T\nu_p$ are the number of delay and Doppler bins, respectively, in the fundamental DD period, where B and T denote the bandwidth and time duration of the pulsone, respectively.

We define $\mathbb{K} = \{0,\cdots,M-1\}$ and $\mathbb{L} = \{0,\cdots,N-1\}$. Information symbols $x[k,l], k \in \mathbb{K}, l \in \mathbb{L}$, drawn from a modulation alphabet $\mathbb{A}$, are multiplexed onto the DD information lattice $\Lambda_{\rm dd}$. The resulting discrete information signal in the DD domain is quasi-periodic with delay period M and Doppler period N, represented as

$$x_{\rm dd}[k+nM, l+mN] = x[k,l]e^{j2\pi n\frac{l}{N}}, \quad m,n \in \mathbb{Z}. \tag{2}$$

This is lifted to a continuous signal using DD impulses as $x_{\rm dd}(\tau,\nu) = \sum_{k,l\in\mathbb{Z}} x_{\rm dd}[k,l]\delta\left(\tau - k\frac{\tau_p}{M}\right)\delta\left(\nu - l\frac{\nu_p}{N}\right)$. To produce a time- and bandwidth-limited transmit signal, pulse shaping is performed employing twisted convolution operation (denoted by $*_\sigma$)[1] with the DD domain transmit pulse shaping filter $w_{\rm tx}(\tau,\nu)$, i.e., $x_{\rm dd}^{w_{\rm tx}}(\tau,\nu) = w_{\rm tx}(\tau,\nu) *_\sigma x_{\rm dd}(\tau,\nu)$, The TD transmit signal is realized by applying the inverse time-Zak transform[2], given by $s_{\rm td}(t) = \mathcal{Z}_t^{-1}\left(x_{\rm dd}^{w_{\rm tx}}(\tau,\nu)\right)$.

The spreading function represents the doubly dispersive channel in DD domain as

$$h(\tau,\nu) = \sum_{i=1}^{P} h_i\delta(\tau-\tau_i)\delta(\nu-\nu_i), \tag{3}$$

where P denotes the number of paths, and h_i, τ_i, and ν_i denote the complex channel gain, delay shift, and Doppler shift associated with the ith path, respectively. Assuming uniform scattering profile, h_i is assumed to be i.i.d $\mathcal{CN}(0,1/P)$.

Due to the time and frequency dispersion introduced by the channel, the TD received signal at the receiver is expressed as $r_{\rm td}(t) = \iint h(\tau,\nu)s_{\rm td}(t-\tau)e^{j2\pi\nu(t-\tau)}d\tau\, d\nu + n_{\rm td}(t)$, where $n_{\rm td}(t)$ is AWGN. To facilitate signal processing and detection in the DD domain, the received TD signal is transformed using the Zak transform[3] as $y_{\rm dd}(\tau,\nu) = \mathcal{Z}_t\left(r_{\rm td}(t)\right)$. The DD received signal is match-filtered with the DD domain receive pulse shaping filter $w_{\rm rx}(\tau,\nu)$, yielding $y_{\rm dd}^{w_{\rm rx}}(\tau,\nu) = w_{\rm rx}(\tau,\nu) *_\sigma y_{\rm dd}(\tau,\nu)$. This is then sampled on $\Lambda_{\rm dd}$ to get the discrete DD received signal as

$$y_{\rm dd}[k,l] = y_{\rm dd}^{w_{\rm rx}}\Big(\tau = k\frac{\tau_p}{M}, \nu = l\frac{\nu_p}{N}\Big), \quad k,l \in \mathbb{Z}. \tag{4}$$

Then the input-output relation is given by a discrete twisted convolution operation as

$$y_{\rm dd}[k,l] = h_{\rm dd}[k,l] *_\sigma x_{\rm dd}[k,l] + n_{\rm dd}[k,l], \tag{5}$$

where $n_{\rm dd}[k,l]$ is the noise sample and $h_{\rm dd}[k,l]$ denotes the effective channel filter obtained by sampling

$$h_{\rm dd}(\tau,\nu) \triangleq w_{\rm rx}(\tau,\nu) *_\sigma h(\tau,\nu) *_\sigma w_{\rm tx}(\tau,\nu) \tag{6}$$

on $\Lambda_{\rm dd}$. Substituting the definition of twisted convolution in (5), we have the complete input-output relation as

$$y_{\rm dd}[k,l] = \sum_{k',l'\in\mathbb{Z}} h_{\rm dd}[k-k',l-l']x_{\rm dd}[k',l']e^{j2\pi\frac{(l-l')k'}{MN}} + n_{\rm dd}[k,l]. \tag{7}$$

Due to the quasi-periodicity in the DD domain, it suffices to consider received samples within the fundamental period. This allows for a vectorized representation of the MN samples

$$\mathbf{y} = \mathbf{H}\mathbf{x} + \mathbf{n}, \tag{8}$$

where $\mathbf{x},\mathbf{y},\mathbf{n} \in \mathbb{C}^{MN\times 1}$, such that their $(kN+l+1)$th entries are given by $x_{kN+l+1} = x_{\rm dd}[k,l]$, $y_{kN+l+1} = y_{\rm dd}[k,l]$, $n_{kN+l+1} = n_{\rm dd}[k,l]$, and the effective channel matrix $\mathbf{H} \in \mathbb{C}^{MN\times MN}$ whose entries are given as

$$\mathbf{H}[kN+l+1, k'N+l'+1] = \sum_{m,n\in\mathbb{Z}} h_{\rm dd}[k-k'-nM, l-l'-mN]e^{j2\pi\frac{(l-l'-mN)(k'+nM)}{MN}}e^{j2\pi nl'/N}, \tag{9}$$

where $k,k' \in \mathbb{K}$, $l,l' \in \mathbb{L}$.

III. Diversity analysis of Zak-OTFS

In this section, we present the diversity analysis of Zak-OTFS. For this, we introduce an equivalent form of (8) as

$$\mathbf{y} = \mathbf{X}\mathbf{h} + \mathbf{n}, \tag{10}$$

where $\mathbf{h} \in \mathbb{C}^{P\times 1}$ contains the complex channel gains and $\mathbf{X} \in \mathbb{C}^{MN\times P}$ is the transmit symbol matrix corresponding to the transmit symbol vector $\mathbf{x}$, given by

$$\mathbf{X} = \underbrace{\begin{bmatrix}\mathbf{G}_1 & \mathbf{G}_2 & \cdots & \mathbf{G}_P\end{bmatrix}}_{\mathbf{G}}\underbrace{\left(\mathbf{I}_P \otimes \mathbf{x}\right)}_{\tilde{\mathbf{x}}}. \tag{11}$$

The matrix $\mathbf{G}_i \in \mathbb{C}^{MN\times MN}, i = 1,\cdots,P$ corresponding to the ith path depends on the ith path's delay and Doppler shifts, and the transmit and receive pulse shaping filters. It is constructed using the following equations:

$$\mathbf{G}_i[kN+l+1, k'N+l'+1] = \sum_{m,n\in\mathbb{Z}} g_i[k-k'-nM, l-l'-mN]e^{j2\pi\frac{(l-l'-mN)(k'+nM)}{MN}}e^{j2\pi nl'/N}, \tag{12}$$

[1] $x(\tau,\nu) *_\sigma y(\tau,\nu) \triangleq \iint x(\tau',\nu')y(\tau-\tau',\nu-\nu')e^{j2\pi\nu'(\tau-\tau')}d\tau'\, d\nu'$.

[2] $\mathcal{Z}_t^{-1}\left(x(\tau,\nu)\right) \triangleq \sqrt{\tau_p}\int_0^{\nu_p} x(t,\nu)d\nu$.

[3] $\mathcal{Z}_t\left(z(t)\right) \triangleq \sqrt{\tau_p}\sum_{k\in\mathbb{Z}} z(\tau+k\tau_p)e^{-j2\pi\nu k\tau_p}$.

where $k, k' \in \mathbb{K}$, $l, l' \in \mathbb{L}$, and

$$g_i(\tau,\nu) = e^{-j2\pi\nu_i\tau_i} \iint w_{\rm rx}(\tau'-\tau_i,\nu'-\nu_i) \; w_{\rm tx}(\tau-\tau',\nu-\nu')e^{j2\pi\nu'(\tau-\tau'+\tau_i)}d\tau' \, d\nu', \quad (13)$$

$$g_i[k,l] = g_i\Big(\tau = k\frac{\tau_p}{M}, \nu = l\frac{\nu_p}{N}\Big), \quad k,l \in \mathbb{Z}. \quad (14)$$

Assuming normalized transmit symbols such that the SNR $\gamma = 1/\sigma^2$, and perfect DD channel knowledge and ML detection at the receiver, the probability that a transmit symbol vector $\mathbf{x}_i$ be wrongly decoded as $\mathbf{x}_j$ is the pairwise error probability (PEP) between $\mathbf{x}_i$ and $\mathbf{x}_j$, given by[4]

$$\mathrm{P}\left(\mathbf{x}_i \to \mathbf{x}_j \mid \mathbf{h}\right) = \mathrm{Q}\left(\sqrt{\frac{\gamma \left\|(\mathbf{X}_i - \mathbf{X}_j)\mathbf{h}\right\|^2}{2}}\right), \quad (15)$$

where $i, j = 1, \cdots, Q_s$, where $Q_s = |\mathbb{A}|^{MN}$ and $i \neq j$. Since $\mathbf{h} \sim \mathcal{CN}(0, \mathbf{I}_P/P)$, an upper bound for the average PEP can be obtained using the Chernoff bound as

$$\mathrm{P}\left(\mathbf{x}_i \to \mathbf{x}_j\right) \leq \prod_{l=1}^{r} \frac{1}{1+\frac{\gamma\lambda_l^{(ij)}}{4P}}, \quad (16)$$

where r is the rank of difference matrix $\mathbf{\Delta}_{ij} = (\mathbf{X}_i - \mathbf{X}_j)$ and $\lambda_l^{(ij)}, l = 1, \cdots, r$ are the non-zero eigenvalues of $\mathbf{\Delta}_{ij}\mathbf{\Delta}_{ij}^H$. At high SNRs, the equation can be further simplified as

$$\mathrm{P}\left(\mathbf{x}_i \to \mathbf{x}_j\right) \leq \frac{\gamma^{-r}(4P)^r}{\prod_{l=1}^{r}\lambda_l^{(ij)}}. \quad (17)$$

The union bound-based upper bound on the bit error probability can be written as

$$\mathrm{P}_e \leq \frac{1}{Q_s MN \log_2|\mathbb{A}|} \sum_{i=1}^{Q_s}\sum_{j=1, j\neq i}^{Q_s} d\left(\mathbf{x}_i, \mathbf{x}_j\right) \mathrm{P}\left(\mathbf{x}_i \to \mathbf{x}_j\right). \quad (18)$$

where $d\left(\mathbf{x}_i, \mathbf{x}_j\right)$ denotes the Hamming distance between $\mathbf{x}_i$ and $\mathbf{x}_j$. From (17) and (18), it can be observed that the diversity order is given by

$$\rho = \min_{i\neq j} \; \mathrm{rank}(\mathbf{\Delta}_{ij}). \quad (19)$$

Now, use (11) to express the difference matrix $\mathbf{\Delta}_{ij}$ as

$$\mathbf{\Delta}_{ij} = \mathbf{G}\underbrace{\left(\tilde{\mathbf{X}}_i - \tilde{\mathbf{X}}_j\right)}_{\tilde{\mathbf{X}}_{ij}}. \quad (20)$$

Using the rank of product of matrices in [17], we can write

$$\mathrm{rank}\big(\mathbf{\Delta}_{ij}\big) = \mathrm{rank}\big(\tilde{\mathbf{X}}_{ij}\big) - \dim\big(N(\mathbf{G}) \cap R\big(\tilde{\mathbf{X}}_{ij}\big)\big), \quad (21)$$

where $N(\cdot)$ and $R(\cdot)$ denote the null space and range space of a matrix, respectively, and $\dim(\cdot)$ denote the dimension of a vector space. From (20) and (11), we have

$$\tilde{\mathbf{X}}_{ij} = \big(\mathbf{I}_P \otimes (\mathbf{x}_i - \mathbf{x}_j)\big). \quad (22)$$

[4]We note that (15) assumes that the filtered noise samples in the DD domain are i.i.d Gaussian. For Gaussian filter, the noise samples are correlated, and therefore the assumption underlying (15) does not hold. In Fig. 3, this is reflected in the gap between the simulated BER and the analytical upper bound for Gaussian filter derived using this assumption.

It is readily apparent that $\mathrm{rank}(\tilde{\mathbf{X}}_{ij}) = P, \forall i \neq j$. Thus, (21) implies that full rank of difference matrix is obtained when

$$N(\mathbf{G}) \cap R\big(\tilde{\mathbf{X}}_{ij}\big) = \phi, \quad (23)$$

which provides the condition for achieving full diversity. Recall that the matrix $\mathbf{G}$ is populated based on the transmit and receive pulse shaping filters (follows from (12)-(14)). Hence, by appropriate design of the filters that satisfy condition (23) for all $i \neq j$ and thereby ensure full rank for all difference matrices, full DD domain diversity can be extracted. In the results and discussions section (Sec. V), we demonstrate the fulfillment of this condition for sinc and Gaussian filters for various system parameters.

IV. BER ANALYSIS WITH IMPERFECT CSI

In this section, we analyze the bit error performance of Zak-OTFS with imperfect CSI caused due to errors in the estimation of the DD channel coefficients. We derive a closed-form expression for the exact PEP, to establish an upper bound on the BER. Also, we derive the optimum ML rule in case of imperfect CSI. The estimated channel gain $\hat{h}_i$ obtained using pilot based estimation techniques can be written as

$$\hat{h}_i = h_i + e_i, \quad (24)$$

where e_i is the channel estimation error associated with the true channel gain h_i. Consider $\mathbf{e} = [e_1 \; e_2 \; \cdots \; e_P]^{\mathrm{T}} \sim \mathcal{CN}\left(0, \sigma_e^2\mathbf{I}_P\right)$ independent of $\mathbf{h}$ and $\mathbf{n}$, where σ_e^2 is the variance of the channel estimation error, which depends on the estimation technique used. Then, we have

$$\hat{\mathbf{H}} = \mathbf{H} + \mathbf{E}, \quad (25)$$

where $\hat{\mathbf{H}}$ and $\mathbf{E}$ denote the estimated channel matrix and the estimation error matrix, respectively. In the absence of the perfect knowledge of $\mathbf{H}$, using the estimated $\hat{\mathbf{H}}$ in place of $\mathbf{H}$ in the conventional ML decision rule gives the following mismatched ML rule:

$$\hat{\mathbf{x}} = \underset{\mathbf{x}\in\mathbb{A}^{MN\times 1}}{\arg\min} \|\mathbf{y} - \hat{\mathbf{H}}\mathbf{x}\|^2, \quad (26)$$

Assuming all transmit vectors as equally likely, the PEP between $\mathbf{x}_i$ and $\mathbf{x}_j$ as per the decision rule in (26) is given by

$$\mathrm{P}\left(\mathbf{x}_i \to \mathbf{x}_j \mid \hat{\mathbf{H}}\right) = \mathrm{P}\left(\left\|\mathbf{y} - \hat{\mathbf{H}}\mathbf{x}_j\right\|^2 < \|\mathbf{y} - \hat{\mathbf{H}}\mathbf{x}_i\|^2\right). \quad (27)$$

Using (8), (27) can be written as

$$\mathrm{P}\Big(\mathbf{x}_i \to \mathbf{x}_j \mid \hat{\mathbf{H}}\Big) = \mathrm{P}\big(\|\mathbf{H}\left(\mathbf{x}_i - \mathbf{x}_j\right) + \mathbf{n} - \mathbf{E}\mathbf{x}_j\|^2 < \|\mathbf{n} - \mathbf{E}\mathbf{x}_i\|^2\big). \quad (28)$$

Let $\mathbf{a} \triangleq (\mathbf{X}_i - \mathbf{X}_j)\,\mathbf{h} + \mathbf{n} - \mathbf{X}_j\mathbf{e}$ and $\mathbf{b} \triangleq \mathbf{n} - \mathbf{X}_i\mathbf{e}$. Using the vectorized relation in (10) and defining the decision statistic $D = \|\mathbf{a}\|^2 - \|\mathbf{b}\|^2$, we can get the average PEP as

$$\mathrm{P}\left(\mathbf{x}_i \to \mathbf{x}_j\right) = \mathbb{E}_{\mathbf{h},\mathbf{e}}\left\{\mathrm{P}\left(D < 0\right)\right\}. \quad (29)$$

D can be further written in Hermitian quadratic form as $D = \mathbf{q}^H\mathbf{S}\mathbf{q}$, where $\mathbf{q} = \begin{bmatrix}\mathbf{a}^T & \mathbf{b}^T\end{bmatrix}^T$ and $\mathbf{S} = \mathrm{diag}\left(\mathbf{I}_{MN}, -\mathbf{I}_{MN}\right)$. $\mathbf{q}$ is a zero mean vector, whose covariance matrix is given by

$$\mathbf{K}_q = \begin{bmatrix} \sigma_h^2\left(\mathbf{X}_i - \mathbf{X}_j\right)\left(\mathbf{X}_i - \mathbf{X}_j\right)^H + \sigma_e^2\mathbf{X}_j\mathbf{X}_j^H + \sigma^2\mathbf{I}_{MN} & \sigma_e^2\mathbf{X}_j\mathbf{X}_i^H + \sigma^2\mathbf{I}_{MN} \\ \sigma_e^2\mathbf{X}_i\mathbf{X}_j^H + \sigma^2\mathbf{I}_{MN} & \sigma_e^2\mathbf{X}_i\mathbf{X}_i^H + \sigma^2\mathbf{I}_{MN} \end{bmatrix}. \quad (30)$$

where $\sigma_{\rm h}^2 = \mathbb{E}(|h_i|^2) = 1/P, \forall i$. Letting $\mathbf{A} \triangleq \mathbf{K_q S}$, we can write

$$\mathbf{A}=\begin{bmatrix} \sigma_h^2 \left(\mathbf{X}_i - \mathbf{X}_j\right)\left(\mathbf{X}_i - \mathbf{X}_j\right)^H - \left[\sigma_e^2 \mathbf{X}_j \mathbf{X}_i^H + \sigma^2 \mathbf{I}_{MN}\right] \\ \quad + \sigma_e^2 \mathbf{X}_j \mathbf{X}_j{}^H + \sigma^2 \mathbf{I}_{MN} \\ \\ \quad \sigma_e^2 \mathbf{X}_i \mathbf{X}_j{}^H + \sigma^2 \mathbf{I}_{MN} \quad - \left[\sigma_e^2 \mathbf{X}_i \mathbf{X}_i{}^H + \sigma^2 \mathbf{I}_{MN}\right] \end{bmatrix}. \quad (31)$$

Let $\Lambda_1, \Lambda_2, \cdots, \Lambda_{2MN}$ denote the eigenvalues of $\mathbf{A}$. As the decision statistic D is in a Hermitian quadratic form, its characteristic function can be written in closed-form as [12]

$$\begin{aligned} \Phi_D(j\omega) = \mathbb{E}\left[e^{j\omega D}\right] &= \frac{1}{\left|\mathbf{I}_{2MN} - j\omega \mathbf{A}\right|} \\ &= \frac{1}{\prod_{i=1}^{2MN}\left(1 - j\omega\Lambda_i\right)}, \end{aligned} \quad (32)$$

where $j = \sqrt{-1}$. After changing the variable to $z = j\omega$, the exact PEP expression can be obtained from the characteristic function using inversion theorem as [13]-[15]

$$\begin{aligned} \mathrm{P}\left(\mathbf{x}_i \to \mathbf{x}_j\right) = \sum_{l=1}^{K_n} & \frac{(-\lambda_l)^{2MN-c_l}}{\prod_{k=1}^{K_p}\left(\beta_k - \lambda_l\right)^{d_k} \prod_{p\neq l}\left(\lambda_p - \lambda_l\right)^{c_p}} \\ & \times \sum_{\left(q_1, q_2, \cdots, q_{c_l-1}\right)} \prod_{m=1}^{c_l-1} \frac{1}{q_m!} \cdot \frac{1}{m} \left[1 + \left(\sum_{k=1}^{K_p} \frac{d_k \beta_k^m}{\left(\beta_k - \lambda_l\right)^m} \right.\right. \\ & \left.\left. + \sum_{p\neq l} \frac{c_p \lambda_p^m}{\left(\lambda_p - \lambda_l\right)^m}\right)\right]^{q_m}, \end{aligned} \quad (33)$$

where negative eigenvalues of $\mathbf{A}$ are denoted by λ_l having multiplicities $c_l, l = 1, \cdots, K_n$ and the non-negative eigenvalues of $\mathbf{A}$ are denoted by β_k having multiplicities $d_k, k = 1, \cdots, K_p$, such that $\sum_l c_l + \sum_k d_k = 2MN$. Here, K_n and K_p are the number of negative and non-negative eigenvalues, respectively. $q_1, q_2, \cdots, q_{c_l-1}$ are such that $0 \le q_1, q_2, \cdots, q_{c_l-1} \le c_l - 1$ and $\sum_{n=1}^{c_l-1} n q_n = c_l - 1$.

For the case of perfect CSI (i.e., $\sigma_e^2 = 0$), we can analyze the special properties of $\mathbf{A}$ which are revealed by its eigenvalues. If Λ is an eigenvalue of the matrix $\mathbf{A}$, $|\mathbf{A} - \Lambda \mathbf{I}_{2MN}| = 0$. We can write the determinant of block matrices as

$$\left|\begin{bmatrix} \mathbf{B}_1 & \mathbf{B}_2 \\ \mathbf{B}_3 & \mathbf{B}_4 \end{bmatrix}\right| = \left|\mathbf{B}_4\right| \left|\mathbf{B}_1 - \mathbf{B}_2 \mathbf{B}_4^{-1} \mathbf{B}_3\right|, \quad (34)$$

where $\mathbf{B}_1$, $\mathbf{B}_2$, $\mathbf{B}_3$, and $\mathbf{B}_4$ are square matrices of same size and $\mathbf{B}_4$ is invertible. Using this, we get

$$\begin{aligned} \left|\mathbf{A} - \Lambda \mathbf{I}_{2MN}\right| = & \left|\left(\frac{\mathbf{\Delta}_{ij} \mathbf{\Delta}_{ij}^H}{P} + \left(\sigma^2 - \Lambda\right)\mathbf{I}_{MN} - \frac{\sigma^4}{\sigma^2 + \Lambda}\mathbf{I}_{MN}\right)\right| \\ & \times \left|-\left(\sigma^2 + \Lambda\right)\mathbf{I}_{MN}\right|. \end{aligned} \quad (35)$$

Since $\mathbf{\Delta}_{ij}\mathbf{\Delta}_{ij}^H$ is a Hermitian matrix, it is unitarily diagonalizable as $\mathbf{\Delta}_{ij}\mathbf{\Delta}_{ij}^H = \mathbf{U}\mathbf{V}\mathbf{U}^H$, where $\mathbf{U}$ is a unitary matrix and $\mathbf{V}$ has the eigenvalues of the matrix in its diagonal. Also, we can write the identity matrix as $\mathbf{I}_{MN} = \mathbf{U}\mathbf{U}^H$ and $\left|-\left(\sigma^2 + \Lambda\right)\mathbf{I}_{MN}\right| = \left|-\left(\sigma^2 + \Lambda\right)\right|^{MN}$. Substituting these in (35), we get

$$\begin{aligned} \left|\mathbf{A} - \Lambda \mathbf{I}_{2MN}\right| &= \left(-\left(\sigma^2 + \Lambda\right)\right)^{MN} \left|\frac{1}{P}\mathbf{V} - \frac{\Lambda^2}{\sigma^2 + \Lambda}\mathbf{I}_{MN}\right| \\ &= \left[\prod_{l=1}^{P}\left(\Lambda^2 - \frac{v_l}{P}\Lambda - \frac{v_l}{P}\sigma^2\right)\right]\left(\Lambda^2\right)^{MN-P}, \end{aligned} \quad (36)$$

where v_l is the lth element of the diagonal matrix $\mathbf{V}$. The matrix $\mathbf{V}$ has only P non-zero diagonal entries because the $\mathbf{\Delta}_{ij}$ is of size $MN \times P$. From (36), we can see that matrix $\mathbf{A}$ has a zero eigenvalue with multiplicity $2\left(MN - P\right)$ and $2P$ non-zero eigenvalues. When v_ls are distinct and $\mathbf{\Delta}_{ij}$ is full rank[5], i.e., P, we can write the non-zero eigenvalues of $\mathbf{A}$ as

$$\begin{aligned} \lambda_l &= \frac{\frac{v_l}{P} - \sqrt{\frac{v_l^2}{P^2} + \frac{4v_l\sigma^2}{P}}}{2}, \text{ for } l = 1, 2, \cdots, P, \\ \beta_l &= \frac{\frac{v_l}{P} + \sqrt{\frac{v_l^2}{P^2} + \frac{4v_l\sigma^2}{P}}}{2}, \text{ for } l = 1, 2, \cdots, P, \end{aligned} \quad (37)$$

where λ_ls and β_ls are the negative and positive eigenvalues of $\mathbf{A}$, respectively. Now, by substituting $K_n = P$, $K_p = P + 1$, $c_l = 1$ for $l = 1, 2, \cdots, P$, $d_l = 1$ for $l = 1, 2, \cdots, P$, $d_{P+1} = 2(MN - P)$, and $\beta_{P+1} = 0$ in (33), we get

$$\mathrm{P}\left(\mathbf{x}_i \to \mathbf{x}_j\right) = \sum_{l=1}^{P} \frac{(-\lambda_l)^{2P-1}}{\left(\beta_l - \lambda_l\right)\prod_{k\neq l}\left(\beta_k - \lambda_l\right)\left(\lambda_k - \lambda_l\right)}. \quad (38)$$

The above PEP when used in (18) yields the BER upper bound for perfect CSI.

A. True ML detector

This subsection focuses on deriving the optimum decision rule, termed the true ML detector, for imperfect CSI. The true ML detection rule with imperfect CSI is given by

$$\hat{\mathbf{x}} = \underset{\mathbf{x}\in\mathbb{A}^{MN}}{\arg\max}\, \mathrm{P}(\mathbf{y} \mid \hat{\mathbf{H}}, \mathbf{x}). \quad (39)$$

The random vector

$$\begin{bmatrix} \mathbf{h} \\ \hat{\mathbf{h}} \end{bmatrix} = \begin{bmatrix} \mathbf{I}_P & \mathbf{0}_{P\times P} \\ \mathbf{I}_P & \mathbf{I}_P \end{bmatrix} \begin{bmatrix} \mathbf{h} \\ \mathbf{e} \end{bmatrix}, \quad (40)$$

being an affine transformation of $\left[\mathbf{h}^T \ \mathbf{e}^T\right]^T$, is jointly Gaussian. Hence, $\mathbf{h}$ given $\hat{\mathbf{h}}$ is a Gaussian random vector, whose conditional mean is given by $\boldsymbol{\mu}_{\mathbf{h}|\hat{\mathbf{h}}} = \rho^2\hat{\mathbf{h}}$, where $\rho^2 = \sigma_h^2/\left(\sigma_h^2 + \sigma_e^2\right)$ [16]. Using (10), the conditional mean of $\mathbf{y}$ given $\hat{\mathbf{h}}$ and $\mathbf{X}$ can be obtained as

$$\boldsymbol{\mu}_{\mathbf{y}|\hat{\mathbf{H}},\mathbf{x}} = \mathbf{X}\boldsymbol{\mu}_{\mathbf{h}|\hat{\mathbf{h}}} + \mathbb{E}\left[\mathbf{n}\right] = \rho^2\mathbf{X}\hat{\mathbf{h}}. \quad (41)$$

The covariance matrix of $\mathbf{y}$ given $\hat{\mathbf{H}}$ and $\mathbf{x}$ is given by

$$\begin{aligned} \mathbf{C}_{\mathbf{y}|\hat{\mathbf{H}},\mathbf{x}} &= \mathbb{E}\left[\left(\mathbf{y} - \boldsymbol{\mu}_{\mathbf{y}|\hat{\mathbf{H}},\mathbf{x}}\right)\left(\mathbf{y} - \boldsymbol{\mu}_{\mathbf{y}|\hat{\mathbf{H}},\mathbf{x}}\right)^H \mid \hat{\mathbf{H}}, \mathbf{x}\right] \\ &= \sigma^2\mathbf{I}_{MN} + \mathbf{X}\mathbb{E}\left[\left(\mathbf{h} - \rho^2\hat{\mathbf{h}}\right)\left(\mathbf{h} - \rho^2\hat{\mathbf{h}}\right)^H \mid \hat{\mathbf{h}}\right]\mathbf{X}^H \\ &= \sigma^2\mathbf{I}_{MN} + \sigma_h^2\left(1 - \rho^2\right)\mathbf{X}\mathbf{X}^H, \end{aligned} \quad (42)$$

and the psuedo-covariance matrix of $\mathbf{y}$ given $\hat{\mathbf{H}}$ and $\mathbf{x}$ is

$$\begin{aligned} \mathbf{P}_{\mathbf{y}|\hat{\mathbf{H}},\mathbf{x}} &= \mathbb{E}\left[\left(\mathbf{y} - \boldsymbol{\mu}_{\mathbf{y}|\hat{\mathbf{H}},\mathbf{x}}\right)\left(\mathbf{y} - \boldsymbol{\mu}_{\mathbf{y}|\hat{\mathbf{H}},\mathbf{x}}\right)^T \mid \hat{\mathbf{H}}, \mathbf{x}\right] \\ &= \mathbb{E}\left[\mathbf{n}\mathbf{n}^T\right] + \mathbf{X}\mathbb{E}\left[\left(\mathbf{h} - \rho^2\hat{\mathbf{h}}\right)\left(\mathbf{h} - \rho^2\hat{\mathbf{h}}\right)^T \mid \hat{\mathbf{h}}\right]\mathbf{X}^T \\ &= \mathbf{0}_{MN\times MN}. \end{aligned} \quad (43)$$

[5]For the system parameters in Table I, we have observed that all the difference matrices are full rank and also the eigenvalues of the difference matrices are all distinct. Hence, we can use the simplified expression in (38) for these system parameters.

TABLE I: Rank profile of the difference matrices for sinc and Gaussian filters for different system settings/channel profiles.

Profile	System Parameters	Number of difference matrices with rank						
		1	2	3	4	5	6	7
A	$M=2, N=2, \mathbf{P}=\mathbf{2}$ $\tau=[0,0]\Delta\tau,\ \nu=[0,1]\Delta\nu$	0	240	–	–	–	–	–
B	$M=2, N=2, \mathbf{P}=\mathbf{4}$ $\tau=[0,0,1,1]\Delta\tau,\ \nu=[0,1,0,1]\Delta\nu$	0	0	0	240	–	–	–
C	$M=4, N=2, \mathbf{P}=\mathbf{7}$ $\tau=[1,2,3,0,1,2,3]\Delta\tau$ $\nu=[0,0,0,1,1,1,1]\Delta\nu$	0	0	0	0	0	0	65280
D	$M=4, N=2, \mathbf{P}=\mathbf{7}$ $\tau=[1.1,2.9,3.1,0.9,1.1,2.9,3.1]\Delta\tau$ $\nu=[0.9,0.9,0.9,1.1,1.1,1.1,1.1]\Delta\nu$	0	0	0	0	0	0	65280
E	$M=4, N=4, \mathbf{P}=\mathbf{5}$ $\tau=[0,1,1,2,3]\Delta\tau$ $\nu=[0,0,2,3,3]\Delta\nu$	0	0	0	0	4.2949×10^9	–	–

Since $\mathbf{h}$ given $\hat{\mathbf{h}}$ is a complex Gaussian random vector, its pseudo-covariance $\mathbb{E}\left[\left(\mathbf{h}-\rho^2\hat{\mathbf{h}}\right)\left(\mathbf{h}-\rho^2\hat{\mathbf{h}}\right)^T \mid \hat{\mathbf{h}}\right] = \mathbf{0}_{MN\times MN}$, and hence the last step of (43) follows. Therefore, $\mathbf{y}$ given $\hat{\mathbf{H}}$ and $\mathbf{x}$ is a complex Gaussian random vector. Now, writing the system model in real form, (39) becomes

$$\hat{\mathbf{x}} = \underset{\mathbf{x}\in\mathbb{A}^{MN}}{\arg\max}\ |\mathbf{C}_{\mathbf{y}}|^{-\frac{1}{2}} e^{-\frac{1}{2}\mathbf{y}_\mu^T \mathbf{C}_{\mathbf{y}}{}^{-1}\mathbf{y}_\mu}, \tag{44}$$

where

$$\mathbf{y}_\mu = \left[\Re\left\{\mathbf{y}-\boldsymbol{\mu}_{\mathbf{y}|\hat{\mathbf{H}},\mathbf{x}}\right\}, \Im\left\{\mathbf{y}-\boldsymbol{\mu}_{\mathbf{y}|\hat{\mathbf{H}},\mathbf{x}}\right\}\right]^T,$$

$$\mathbf{C}_{\mathbf{y}} = \frac{1}{2}\begin{bmatrix} \Re\left\{\mathbf{C}_{\mathbf{y}|\hat{\mathbf{H}},\mathbf{x}}\right\} & -\Im\left\{\mathbf{C}_{\mathbf{y}|\hat{\mathbf{H}},\mathbf{x}}\right\} \\ \Im\left\{\mathbf{C}_{\mathbf{y}|\hat{\mathbf{H}},\mathbf{x}}\right\} & \Re\left\{\mathbf{C}_{\mathbf{y}|\hat{\mathbf{H}},\mathbf{x}}\right\} \end{bmatrix},$$

and $\Re(\cdot)$ and $\Im(\cdot)$, are the real and imaginary parts, respectively. Equation (44) represents the optimal detection rule under imperfect CSI by incorporating the CSI error statistics into the detection process.

V. Results and Discussions

This section presents the results of the diversity and BER performance of Zak-OTFS obtained through analysis and simulations. We fix the Doppler period of the pulsone at $\nu_p = 3.75$ kHz, resulting in a corresponding delay period $\tau_p = 1/\nu_p = 0.27$ ms. The various system parameters considered are given in Table I, where $\Delta\tau = \frac{\tau_p}{M}$ and $\Delta\nu = \frac{\nu_p}{N}$ are the delay and Doppler resolutions, respectively. Corresponding frame duration and bandwidth are given by $T = N\tau_p$ and $B = M\nu_p$, respectively. These system parameters ensure that the system operates in the crystalline regime i.e., τ_p and ν_p values are greater than the maximum delay (0.209 ms) and maximum Doppler spread (2.8125 kHz), respectively, in the considered channel profiles. BPSK modulation is employed. Sinc and Gaussian pulse shaping filters are used at the transmitter with identical filtering at the receiver (i.e., $w_{\text{tx}}(\tau,\nu) = w_{\text{rx}}(\tau,\nu)$). The sinc filter is given by

$$w_{\text{tx}}(\tau,\nu) = \sqrt{BT}\ \text{sinc}(B\tau)\ \text{sinc}(T\nu),$$

and the Gaussian filter is given by

$$w_{\text{tx}}(\tau,\nu) = \left(\frac{2\alpha_\tau B^2}{\pi}\right)^{\frac{1}{4}} e^{-\alpha_\tau B^2\tau^2} \left(\frac{2\alpha_\nu T^2}{\pi}\right)^{\frac{1}{4}} e^{-\alpha_\nu T^2\nu^2},$$

where we set $\alpha_\tau = \alpha_\nu = 1.584$ to ensure 99% energy localization without time or bandwidth expansion. Also, we demonstrate the diversity results for small frame sizes since simulation of ML detection becomes prohibitively complex for large frame sizes.

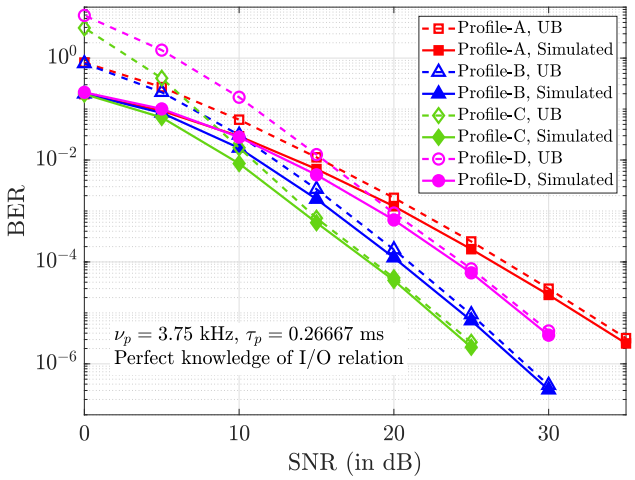

Fig. 2: BER performance of Zak-OTFS with perfect CSI for sinc pulse and different system settings/channel profiles.

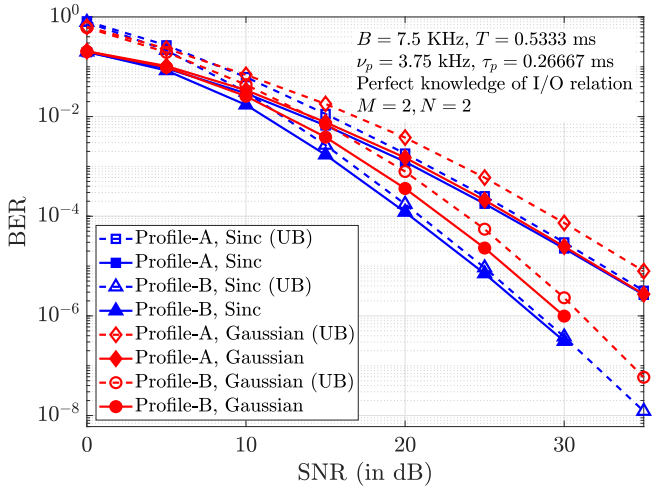

Fig. 3: BER performance of Zak-OTFS for Profiles A and B, sinc and Gaussian filters, and perfect CSI.

Figure 2 shows the simulated BER as well as the BER upper bounds for the considered system settings/channel profiles given in Table I under perfect CSI and sinc pulse. The upper bounds are tight at high SNRs, validating the performance analysis. We observe that the diversity slope (i.e., slope of the BER vs SNR curve in the high SNR regime) increases with increasing P. We assess the diversity order of the considered systems through computation of the rank profile of the difference matrices and the diversity slopes in the BER vs SNR curves. To obtain the rank profile of the difference matrices, we exhaustively enumerate $\tilde{\mathbf{X}}_{ij}$s and construct the $\mathbf{G}$ matrix for various system parameters given in Table I with sinc and Gaussian filters. It revealed that, for each case, condition (23) holds true $\forall i \neq j$, resulting in full rank of all the $Q_s\,(Q_s-1)$ difference matrices, i.e., $\text{rank}(\boldsymbol{\Delta}_{ij}) = P, \forall i \neq j$, implying the extraction of full DD diversity. This can be seen

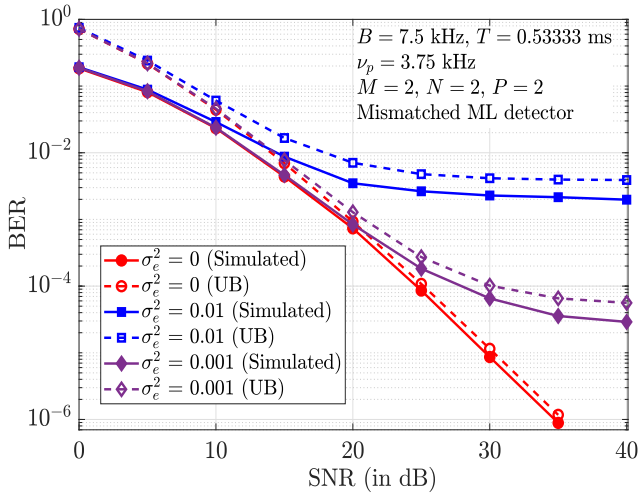

Fig. 4: BER performance of Zak-OTFS with mismatched ML detector for Profile-A, sinc filter, and imperfect CSI.

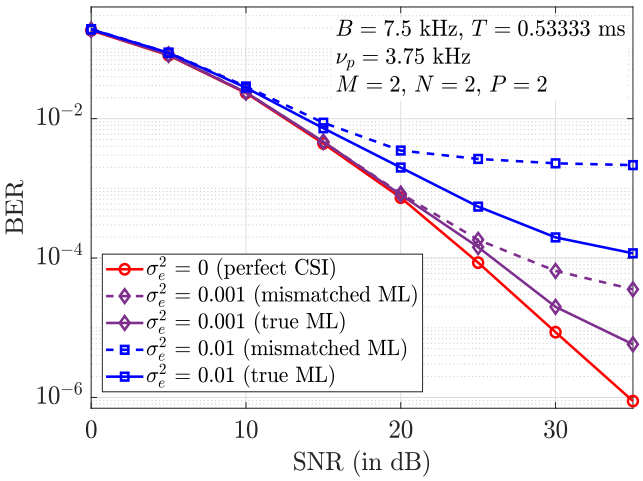

Fig. 5: BER performance comparison between true ML and mismatched ML detectors for Profile-A with sinc filter and imperfect CSI.

from the rank profiles of the difference matrices in Table I. For example, for Profile-A with $M = N = 2$ and $P = 2$, all the $Q_s(Q_s - 1) = 240$ difference matrices are of full rank two. This is corroborated by the diversity slope of two for Profile-A in the SNR vs BER curve in Fig. 3 for both sinc and Gaussian filters. Likewise, for Profile-B with $M = N = 2$ and $P = 4$, all the 240 difference matrices have full rank four (see Table I) and this is corroborated by the corresponding diversity slope in Fig. 3. Hence, we see that Zak-OTFS with sinc and Gaussian filters achieves full diversity satisfying the condition in (23).

Next, in Figs. 4 and 5, we present the BER performance of Zak-OTFS with imperfect CSI and sinc filter. Figure 4 shows the simulated BER plots along with the corresponding upper bounds for Profile-A with different estimation error variances σ_e^2 under mismatched ML detection in (26). Here, the BER performance degrades with an increase in estimation error variance. We can also observe the bit error performance under imperfect CSI floors at high SNRs. In Fig. 5, we compare the BER performance of the true ML detector derived in (44) with that of the mismatched ML detector in (26). We can see that the true ML detector outperforms the mismatched ML, e.g., an improvement of one order of BER when $\sigma_e^2 = 0.01$. This is because the mismatched ML detection rule does not consider estimation error statistics for deriving the detection rule, whereas the true ML detector does.

VI. Conclusions

In this paper, we analyzed the diversity performance of Zak-OTFS using rank criterion and established a necessary condition for the design of pulse shaping filters to achieve full DD diversity. Our simulation results showed that sinc and Gaussian filters achieve the full DD diversity for various channel profiles. Furthermore, we explored the bit error performance of Zak-OTFS under imperfect CSI, analyzing both the mismatched ML detector and the true ML detector which incorporates CSI error statistics.

References

[1] R. Hadani *et al.*, "Orthogonal time frequency space modulation," *Proc. IEEE WCNC'2017*, pp. 1-6, Mar. 2017.

[2] Y. Hong, T. Thaj, and E. Viterbo, *Delay-Doppler Communications: Principles and Applications*, Academic Press, 2022.

[3] A. J. E. M. Janssen, "The Zak transform: A signal transform for sampled time-continuous signals," *Philips J. Res.*, vol. 43, pp. 23-69, 1988.

[4] S. K. Mohammed, "Derivation of OTFS modulation from first principles," *IEEE Trans. Veh. Tech.*, vol. 70, no. 8, pp. 7619-7636, Aug. 2021.

[5] S. K. Mohammed, R. Hadani, A. Chockalingam, and R. Calderbank, "OTFS - a mathematical foundation for communication and radar sensing in the delay-Doppler domain," *IEEE BITS the Information Theory Magazine*, vol. 2, no. 2, pp. 36-55, 1 Nov. 2022.

[6] S. K. Mohammed, R. Hadani, A. Chockalingam, and R. Calderbank, "OTFS — predictability in the delay-Doppler domain and its value to communication and radar sensing," *IEEE BITS the Inform. Theory Mag.*, vol. 3, no. 2, pp. 7-31, Jun. 2023.

[7] F. Jesbin and A. Chockalingam, "Near-optimal detection of Zak-OTFS signals," *Proc. IEEE ICC'2024*, pp. 4476-4481, Jun. 2024.

[8] S. Li, W. Yuan, Z. Wei, J. Yuan, B. Bai, and G. Caire, "On the pulse shaping for delay-Doppler communications," *IEEE GLOBECOM'2023*, pp. 4909-4914, Dec. 2023.

[9] S. Gopalam, I. B. Collings, S. V. Hanly, H. Inaltekin, S. R. B. Pillai, and P. Whiting, "Zak-OTFS implementation via time and frequency windowing," *IEEE Trans. Commun.*, vol. 72, no. 7, pp. 3873-3889, Jul. 2024.

[10] S. Gopalam, H. Inaltekin, I. B. Collings, and S. V. Hanly, "Optimal Zak-OTFS receiver and its relation to the radar matched filter," *IEEE Open J. of the Commun. Soc.*, vol. 5, pp. 4462-4482, 2024.

[11] G. D. Surabhi, R. M. Augustine, and A. Chockalingam, "On the diversity of uncoded OTFS modulation in doubly-dispersive channels," *IEEE Trans. Wireless Commun.*, vol. 18, no. 6, pp. 3049-3063, Jun. 2019.

[12] G. L. Turin, "The characteristic function of Hermitian quadratic forms in complex normal variables," *Biometrika*, vol. 47, nos. 1/2, pp. 199–201, Jun. 1960.

[13] J. Gil-Pelaez, "Note on the inversion theorem," *Biometrika*, vol. 38, pp. 481–482, 1951.

[14] C.-J. de la Vallee Poussin, *Cours D'Analyze Infinitesimale*, 12th ed, Paris: Gauthier-Villars, Libraire Universitaire Louvain, 1959, vol. 1.

[15] P. Garg, R. K. Mallik, and H. M. Gupta, "Performance analysis of space time coding with imperfect channel estimation," *IEEE Trans. Wireless Commun.*, vol. 4, no. 1, pp. 257-265, Jan. 2005.

[16] D. P. Bertsekas and J. N. Tsitsiklis, *Introduction to Probability*, 2nd ed., Belmont, MA, USA: Athena Sci., 2002.

[17] C. D. Meyer, *Matrix Analysis and Applied Linear Algebra*, SIAM, 2001.